Author/s:
Chan, W-S;Li, JS-H;Zhou, KQ;Zhou, R

Title:
Towards a large and liquid longevity market: A graphical population basis risk metric

Date:
2016

Citation:
Chan, W. -S., Li, J. S. -H., Zhou, K. Q. & Zhou, R. (2016). Towards a large and liquid longevity market: A graphical population basis risk metric. Geneva Papers on Risk and Insurance: Issues and Practice, 41 (1), pp.118-127. https://doi.org/10.1057/gpp.2015.9.

Persistent Link:
https://hdl.handle.net/11343/355001

Towards a Large and Liquid Longevity Market: A Graphical Population Basis Risk Metric

Wai-Sum Chan[a], Johnny S.-H. Li[b], Kenneth Q. Zhou[b] and Rui Zhou[c]

[a]Department of Finance, The Chinese University of Hong Kong, Hong Kong.
E-mail: chanws@cuhk.edu.hk
[b]Department of Statistics and Actuarial Science, University of Waterloo, Canada.
E-mails: shli@uwaterlo.ca; q23zhou@uwaterloo.ca
[c]Warren Centre for Actuarial Studies and Research, University of Manitoba, Canada.
E-mail: Rui.Zhou@umanitoba.ca

Pension plan sponsors and annuity providers can offload their longevity risk exposures by trading securities that are linked to broad-based mortality indexes. However, a hedge constructed in this way is subject to population basis risk, arising from the difference in mortality improvements between the hedger's population and the reference population to which the security is linked. To address this problem, which is believed to be a major obstacle to market development, in this paper we contribute a graphical population basis risk metric. The graphical metric allows market participants to not only visually evaluate the extent of population basis risk, but also determine the most appropriate reference population. We illustrate this concept with a hypothetical example.

Keywords: basis risk; longevity risk; prediction regions

Introduction

Rapid, unexpected increases in human life expectancy have posed what is known as longevity risk. On a macroeconomic level, longevity risk affects current account [1], GDP [2] and productivity [3]. From a microeconomic viewpoint, longevity risk undermines the profits and growth opportunities of corporations offering defined-benefit pension schemes, ultimately affecting their share prices. According to IMF [4], if individuals live three years longer than expected, then the already large pension costs would increase by 50% of the 2010 GDP in advanced economies and 25% of the 2010 GDP in emerging economies.

Recently, some pension plan sponsors and annuity providers have chosen to offload longevity risk from their balance sheets. One way to accomplish this act is by transferring

[1]Lee and Mason (2010).
[2]Skirbekk (2004).
[3]van Groezen *et al.* (2005).
[4]International Monetary Fund (2012).

the risk to capital markets, through standardized derivative securities that are linked to broad-based mortality indexes. The first of such transactions occurred in 2008 when Lucida PLC passed part of its longevity risk exposure onto J.P. Morgan by means of a mortality (q-) forward contract. The risk was subsequently transferred to various institutional investors, who accepted the risk exposure for a risk premium.[5] Compared to other risk transfer methods such as reinsurance, capital markets solutions are advantageous in terms of being less costly and having, in theory, no capacity constraint.[6]

Nevertheless, at this point the market for standardized mortality-linked securities is small and lacks liquidity. The industry leaders believe that one major obstacle to market development is an inadequate understanding of population basis risk, the residual risk that originates from the difference in mortality improvements between the hedger's population and the reference population to which the security (hedging instrument) is linked.[7] This problem has been studied by several researchers, who quantified the risk by numerical metrics including percentage reduction in expected shortfall [8], percentage reduction in variance [9] and minimal required buffer [10]. However, as the existing methods cannot be easily communicated to market participants, they still cannot meet the industry's need for a simple, intuitive metric for population basis risk.

To aid in filling this gap, in this paper we contribute a graphical risk metric for assessing population basis risk. The graphical risk metric is constructed from a series of joint prediction regions, allowing users to visually evaluate the ranges of possible outcomes at various confidence levels. Our contribution also enables hedgers to determine, out of all available reference populations, the population that results in the minimum amount of population basis risk. We believe that our contribution is likely to gain wide acceptance among practitioners, who are increasing relying on graphical methods such as survivor fan charts[11], longevity fan charts[12] and heat maps of mortality improvement rates[13] in making their risk management decisions.

We explain the construction of the graphical population basis risk metric in the next section, followed by a section that includes a demonstration based on a hypothetical example

[5]Blake *et al.* (2013).

[6]Cummins and Trainar (2009).

[7]Life and Longevity Markets Association (LLMA) (2012).

[8]Ngai and Sherris (2011).

[9]Cairns *et al.* (2014), Li and Hardy (2011), and Li and Luo (2012).

[10]Stevens *et al.* (2011). The minimal required buffer refers to the minimum asset value (in excess of the best estimate value of the liabilities) such that the probability that the insurer or pension fund will be able to pay all future liabilities is sufficiently high.

[11]Blake *et al.* (2008).

[12]Dowd *et al.* (2010).

[13]Continuous Mortality Investigation Bureau (2009).

and real mortality data. Finally the last section concludes the paper with some suggestions for future research.

Methodology

Let us consider a pension plan whose liability value is proportional to a random survivor index, $S^{(H)}$, where H represents the population of individuals associated with the plan. To hedge its longevity risk exposure, the plan trades a mortality derivative, whose payoff is proportional to another random survivor index, $S^{(R)}$, where R denotes the derivative's reference population. We let $I^{(H)} = S^{(H)} - E(S^{(H)})$ and $I^{(R)} = S^{(R)} - E(S^{(R)})$ be the exceedances of $S^{(H)}$ and $S^{(R)}$ over their expected values, respectively. We base the graphical risk metric on $I^{(H)}$ and $I^{(R)}$ rather than $S^{(H)}$ and $S^{(R)}$, partly because users' primary interest are the possible deviations from the expected outcomes, and partly because the use of $I^{(H)}$ and $I^{(R)}$ ensures all resulting risk metrics are centered at the origin, thereby allowing users to compare the risk metrics for different reference populations readily.

The first step in constructing the graphical population basis risk metric is to simulate realizations of $I^{(H)}$ and $I^{(R)}$ from a multi-population stochastic mortality model, examples of which include the augmented common factor model [14] and the gravity model [15]. Such a model incorporates the correlation between the uncertain mortality improvements of the populations being modeled, and exhibits mean-reversion to avoid resulting in anti-intuitive diverging long-term mortality forecasts.

The second step is to optimize the longevity hedge. We consider a static hedge, which seems more feasible than a dynamic hedge in today's market for longevity risk transfers [16]. Specifically, we aim to find, per dollar amount of the pension liability, the notional amount $h^{(R)}$ of the mortality derivative that would lead to a perfect hedge in the ideal situation when population basis risk is absent, i.e., when $I^{(H)}$ and $I^{(R)}$ are perfectly correlated. We find $h^{(R)}$ by a linear approximation, which implies $h^{(R)} = \frac{\partial I^{(H)}}{\partial I^{(R)}}$. The value of $h^{(R)}$ is estimated by the slope of the first order linear regression of $I^{(H)}$ on $I^{(R)}$, derived from the simulated values of $I^{(H)}$ and $I^{(R)}$ obtained in the first step.

Our choice of $h^{(R)}$, which can be expressed as

$$h^{(R)} = \frac{\text{Cov}(I^{(R)}, I^{(H)})}{\text{Var}(I^{(H)})},$$

[14] Li and Lee (2005).

[15] Dowd *et al*. (2011).

[16] Static hedging is more realistic, because dynamic hedging requires liquid longevity-linked securities that are not yet available in the current market for longevity risk transfers. See Fung et al. (2014).

is justified in the sense that it minimizes the variance of the hedged portfolio; that is, $h^{(R)}$ is the value of h that minimizes the following expression:

$$\begin{aligned}\text{Var}(I^{(H)} - hI^{(R)}) &= \text{Var}(I^{(H)}) + h^2\text{Var}(I^{(R)}) - 2h\text{Cov}(I^{(H)}, I^{(R)}) \\ &= \text{Var}(I^{(R)})\left(h - \frac{\text{Cov}(I^{(H)}, I^{(R)})}{\text{Var}(I^{(R)})}\right) + c,\end{aligned}$$

where c is a constant that is free of h.

Of course, when population basis risk is actually present in reality, $I^{(H)}$ is not necessarily equal to $h^{(R)}I^{(R)}$. If $I^{(H)} > h^{(R)}I^{(R)}$, then the pension liability is under-hedged, and if $I^{(H)} < h^{(R)}I^{(R)}$, then the opposite is true. Population basis risk can therefore be understood as the variability associated with the random deviations between $I^{(H)}$ and $h^{(R)}I^{(R)}$.

The third step is to express the uncertainty surrounding $I^{(H)}$ and $h^{(R)}I^{(R)}$ by a series of joint prediction regions. Mathematically, $\mathbf{J}_\alpha$ is a joint prediction region for the duplet $(I^{(H)}, h^{(R)}I^{(R)})$ with coverage probability $0 < 1 - \alpha \leq 1$ if

$$\Pr((I^{(H)}, h^{(R)}I^{(R)}) \in \mathbf{J}_\alpha) = 1 - \alpha.$$

The region $\mathbf{J}_\alpha$ should encompass $100(1 - \alpha)\%$ of the possible combinations of $I^{(H)}$ and $h^{(R)}I^{(R)}$. For a given value of α, a larger $\mathbf{J}_\alpha$ reflects a higher amount of population basis risk. We construct nine joint prediction regions, with $\alpha = 0.1, 0.2, \ldots, 0.9$.

Finally, the graphical risk metric is created by plotting on a Cartesian coordinate plane the 10% joint prediction region with the darkest shading, surrounded by the 20%, 30%, ..., 90% joint prediction regions with progressively lighter shadings. From the areas of the prediction regions and the degrees of shading, one can visualize ranges of possible hedging outcomes and their associated probabilities of occurrence. The proposed risk metric is somewhat similar to the well-known Bank of England inflation fan chart, which simultaneously depicts interval forecasts of future inflation rates at different confidence levels by using different shades of colour.[17] It also has a close resemblance to the existing survivor/longevity fan charts.[18]

An Illustration

We now illustrate the graphical population basis risk metric with a hypothetical example. Let us suppose that H, the population associated with the pension plan (the hedger), is Canadian males. Suppose further that at the time when the hedge is established, there is no mortality

[17] Wallis (2003).
[18] Blake *et al.* (2008) and Dowd *et al.* (2010).

derivative linked to Canadian males. However, the plan may use a mortality derivative that is linked to an alternative reference population (R), which can be either U.S. males, German males, Dutch males, or English and Welsh males.[19]

The survivor index used is the *ex post* probability that an individual currently aged 65 will survive to age 90:

$$S^{(i)} = \prod_{t=0}^{24}(1 - q(65+t, t, i)), \qquad i = H, R,$$

where $q(x,t,i)$ is the probability that an individual from population i dies in year t, given that the individual is alive and aged x at the beginning of year t. This survivor index is very similar to the one that is associated with the 25-year longevity bond that was announced by BNP Paribas and the European Investment Bank in 2004.[20]

We use the augmented common factor model proposed by Li and Lee[21] to concurrently model the future mortality of all five populations. The model can be expressed as

$$\ln(m(x,t,i)) = a(x,i) + B(x)K(t) + b(x,i)k(t,i) + \epsilon(x,t,i), \quad i = H, R,$$

where $m(x,t,i)$ denotes population i's central death rate at age x and in year t, $a(x,i)$ is a parameter measuring population i's average level of mortality at age x, $K(t)$ is a time-varying index that is shared by all populations being modeled, $k(t,i)$ is the time-varying index that is specific to population i, parameters $B(x)$ and $b(x,i)$ respectively reflect the sensitivity to $K(t)$ and $k(x,i)$ at age x, and $\epsilon(x,t,i)$ is the error term.

Following Li and Lee, we estimate $a(x,i)$ by setting it to the average of $\ln(m(x,t,i))$ over the data sample period. To estimate $B(x)$ and $K(t)$, we apply a first order singular value decomposition (SVD) to the matrix of $\sum_i w(x,t,i)(\ln(m(x,t,i)) - \hat{a}(x,i))$, where $w(x,t,i)$ represents population i's number of exposures at age x and year t and the ˆ sign denotes an estimate. Another first order SVD is applied to the matrix of $\ln(m(x,t,i)) - \hat{a}(x,i) - \hat{B}(x)\hat{K}(t)$ to obtain estimates of parameters $b(x,i)$ and $k(t,i)$.

The evolution of $K(t)$ over time is modeled by a random walk with drift:

$$K(t) = C + K(t-1) + \xi(t),$$

where C is the drift term and $\{\xi(t)\}$ is a sequence of i.i.d. normal random variables with zero mean and constant variance, whereas the evolution of $k(t,i)$ over time is modeled by a

[19] As a matter of fact, the LLMA (www.llma.org) provides mortality indexes for these four national populations. Derivative securities can be written on LLMA's mortality indexes.

[20] See Blake *et al.* (2013).

[21] Li and Lee (2005).

Population	$h^{(R)}$
The US	1.3121
Germany	1.3804
The Netherlands	1.3718
England and Wales	1.3203

Table 1: The calculated values of $h^{(R)}$ for the four reference populations under consideration.

first order autoregressive process:

$$k(t,i) = \phi_0(i) + \phi_1(i)k(t-1,i) + \zeta(t,i),$$

where $\phi_0(i)$ is a constant, $\phi_1(i)$ is another constant whose absolute value is strictly less than one, and $\{\zeta(t,i)\}$ is a sequence of i.i.d. normal random variables with zero mean and constant variance. The process for $k(t,i)$ is mean-reverting, so that the projected mortality rates for different populations do not diverge indefinitely over time.

The model is fitted to historical data covering the age range of 60 to 89 and the sample period of 1960 to 2009. Most of the required data are obtained from the Human Mortality Database.[22] The only exception is the data for German males prior to 1991 (when the Berlin Wall fell), which are obtained from the LLMA.[23]

Under the augmented common factor model, the probability distribution of $S^{(i)}$ cannot be written in closed-form; thus, the joint prediction regions cannot be derived analytically as was done by Chan *et al*.[24] Instead, we obtain the joint prediction regions with the following numerical procedure:

1. Simulate 50,000 future values of $m(x,t,i)$ from the estimated augmented common factor model. Using these simulated values and the approximation $q(x,t,i) = 1 - \exp(-m(x,t,i))$,[25] calculate realizations of $I^{(H)}$ and $I^{(R)}$.

2. Using the realized values of $I^{(H)}$ and $I^{(R)}$, calculate the value of $h^{(R)}$ using the previously described linear regression methodology. The calculated values of $h^{(R)}$ for the four reference populations under consideration are displayed in Table 1.

3. Let $Y = (I^{(H)}, h^{(R)}I^{(R)})'$. For each simulated realization of Y, calculate its Mahalanobis distance to the best estimate as $Y'\hat{S}^{-1}Y$, where $\hat{S}$ is the sample covariance

[22] Human Mortality Database (2014).
[23] http://www.llma.org/Index-Data.html
[24] Chan *et al*. (2014).
[25] The approximation is exact if the force of mortality between two integer ages is constant.

matrix of Y. Note that the best estimate of Y is $\text{E}(Y) = (0, 0)'$. Geometrically speaking, the Mahalanobis distance may be viewed as the physical distance between the realization of Y and the origin, weighted by the standard deviations and covariance of $I^{(H)}$ and $h^{(R)}I^{(R)}$.[26]

4. Sort the 50,000 simulated realizations by their Mahalanobis distances to the best estimate. Choose the $50,000(1 - \alpha)$ realizations with the shortest Mahalanobis distances.

5. Draw a convex hull to enclose the $50,000(1 - \alpha)$ chosen realizations. In geometrical terms, the convex hull is the smallest convex set that contains the selected $50,000(1 - \alpha)$ pairs of $I^{(H)}$ and $h^{(R)}I^{(R)}$.

The convex hull drawn is a $100(1-\alpha)\%$ joint prediction region for $I^{(H)}$ and $h^{(R)}I^{(R)}$, because by construction it contains a randomly selected pair of $I^{(H)}$ and $h^{(R)}I^{(R)}$ in the simulated sample with a probability of $1 - \alpha$. The use of a convex hull (the smallest convex set) prevents the joint prediction region from overstating the underlying uncertainty.

Figure 1 shows the graphical population basis risk metric when the reference population is English and Welsh males. The two dotted lines divide the diagram into four quadrants. The upper-right (lower-left) quadrant contains the outcomes when future mortality of both populations improves faster (slower) than expected, while the upper-left (lower-right) quadrant encompasses the outcomes when the mortality of Canadian males improves slower (faster) than expected and the mortality of English and Welsh males improves faster (slower) than expected. The dots in the diagram represent the 50,000 simulated pairs of $I^{(H)}$ and $h^{(R)}I^{(R)}$. These dots should align perfectly on the 45-degree line in the ideal case when there is no population basis risk. The region below the 45-degree line contains the under-hedging outcomes, while the region above contains the over-hedging outcomes. The vertical (or equivalently, horizontal) distance from an outcome to the 45-degree line indicates the extent of over- or under-hedging associated with that outcome. The likelihood of an outcome is visible from the colour shade of the region in which the outcome is located. Essentially, the darker the shading, the more likely the outcome.

The area spanned by the risk metric indicates the overall level of population basis risk. Therefore, one may determine the reference population that leads to the minimum amount of basis risk by comparing the areas of the risk metrics for all available reference populations. Figure 2 displays the graphical risk metrics for all four reference populations under consideration. It is clear that the risk metric for U.S. males is smaller than the risk metrics for the

[26] See Gnanadesikan and Kettenring (1972) for further information about Mahalanobis distances.

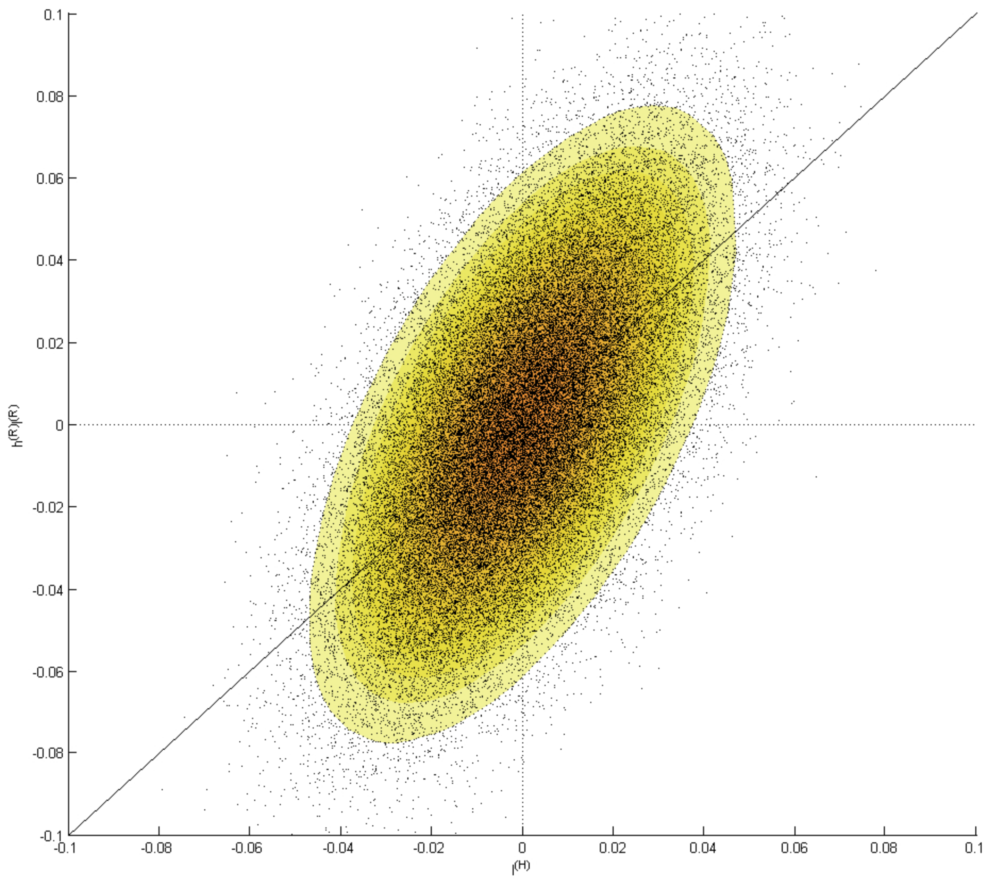

Figure 1: The graphical population basis risk metric for the situation when the hedger's population (H) is Canadian males and the derivative's reference population (R) is English and Welsh males. The dots represent the 50,000 simulated pairs of $I^{(H)}$ and $h^{(R)}I^{(R)}$.

other three available reference populations. Hence, for this hypothetical example, the hedger should choose to trade a derivative that is linked to U.S. male mortality.

Conclusion

In this paper, we have proposed a graphical metric to intuitively communicate information about the level of population basis risk that an index-based longevity hedge is exposed to. The graphical risk metric is composed of a series of joint prediction regions of possible hedging outcomes, which are simulated from an assumed multi-population stochastic mortality model. Various aspects of population basis risk are reflected in the graphical risk metric. First, the area of a prediction region indicates the overall level of the population basis risk. Second, the shade of a prediction region reflects the likelihood of the hedging outcomes enclosed by the region. Third, the shape of the prediction region reveals how the hedger's liability is correlated with the survivor index to which the standardized hedging instrument is linked.

Compared to existing population basis risk metrics which are mostly numerical and only measure the overall risk level, the proposed metric is more informative in that it captures more aspects of population basis risk. Along with the existing numerical metrics, the proposed graphical metric may help potential hedgers better understand population basis risk and hence make their risk management decisions.

We have also illustrated the graphical population basis risk metric by a hypothetical example, in which the hedger's liability is associated with Canadian mortality while the available hedging instruments are linked respectively to the populations of the U.S., Germany, the Netherlands and England and Wales. Given the resulting joint prediction regions, one can easily tell that among the four reference populations, the U.S. is the most appropriate for the hypothetical hedger. We believe that as the market grows and standardized instruments linked to different reference populations become available, the proposed technique can assist hedgers with their choices of hedging instruments.

The graphical population basis risk metric depends on the assumed multi-population stochastic mortality model. Admittedly, the conclusions derived from the graphical metric may turn out to be different if another stochastic mortality model is assumed. It is warranted to explore in future work the robustness of the graphical risk metric relative to model choices. From a practical viewpoint, it would be useful to incorporate the proposed technique into existing stochastic mortality modeling software such as the LLMA's LifeMetrics. Such a development would allow potential hedgers to customize the graphical population basis risk metric on the basis of their own choices of mortality models and data sets.

Acknowledgements

This work is supported by research grants from the Global Risk Institute, the Natural Science and Engineering Research Council of Canada, the Society of Actuaries Center of Actuarial Excellence Program, and the Research Grants Council of the Hong Kong Special Administrative Region (General Research Fund Project No. CUHK 440812H).

References

Blake, D., Cairns, A., Coughlan, G., Dowd, K. and MacMinn, R. (2013) 'The new life market', *Journal of Risk and Insurance* 80(3): 501–557.

Blake, D., Cairns, A.J.G. and Dowd, K. (2008). 'Longevity risk and the Grim Reaper's toxic tail: the survivor fan charts', *Insurance: Mathematics and Economics* 42: 1062-1066.

Cairns, A.J.G., Blake, D., Dowd, K. and Coughlan, G.D. (2014) 'Longevity hedge effectiveness: a decomposition', *Quantitative Finance* 14(2): 217–235.

Chan, W.S., Li, J.S.-H. and Li, J. (2014) 'The CBD mortality indexes: modeling and applications', *North American Actuarial Journal* 18(1): 38–58.

Continuous Mortality Investigation Bureau (2009). 'A prototype mortality projections model: Part two - detailed analysis', Continuous Mortality Investigation Working Paper 39.

Cummins, J.D. and Trainar, P. (2009) 'Securitization, insurance, and reinsurance', *Journal of Risk and Insurance* 76(3): 463–492.

Dowd, K., Blake, D. and Cairns, A.J.G. (2010). 'Facing up to uncertain life expectancy: the longevity fan charts', *Demography* 47: 67-78.

Dowd, K., Cairns, A.J.G., Blake, D., Coughlan, G.D., Epstein, D. and Khalaf-Allah, M. (2011) 'A gravity model of mortality rates for two related populations', *North American Actuarial Journal* 15(2): 334–356.

Fung, M.C., Ignatieva, K. and Sherris, M. (2014). 'Systematic mortality risk: An analysis of guaranteed lifetime withdrawal benefits in variable annuities', *Insurance Mathematics and Economics* 58: 103–115.

Gnanadesikan, R. and Kettenring, J.R. (1972). 'Robust estimates, residuals, and outlier detection with multiresponse data', *Biometrics* 28(1) 81–124

Human Mortality Database, University of California, Berkeley, USA; and Max Planck Institute for Demographic Research, Germany (2014) Available at www.mortality.org (assessed 1 March 2014).

International Monetary Fund (2012) *Global financial stability report: the quest for lasting stability*, Washington, DC: International Monetary Fund.

Lee, R. and Mason, A. (2010) 'Some macroeconomic aspects of global population aging', *Demography* 47: S151–172.

Li, J.S.-H. and Hardy, M.R. (2011) ' Measuring basis risk in longevity hedges', *North American Actuarial Journal* 15(2): 177–200.

Li, J.S.-H. and Luo, A. (2012) 'Key q-duration: a framework for hedging longevity risk', *ASTIN Bulletin* 42(2): 413–452.

Li, N. and Lee, R. (2005) 'Coherent mortality forecasts for a group of populations: an Extension of the Lee-Carter method', *Demography* 42(3): 575–594.

LLMA (2012) ' Basis risk in longevity hedging: parallels with the past'. *Institutional Investors Journal*, 2012(1): 39–45.

Ngai, A. and Sherris, M. (2011). 'Longevity risk management for life and variable annuities: The effectiveness of static hedging using longevity bonds and derivatives', *Insurance Mathematics and Economics* 49(1): 100–114.

Skirbekk, V. (2004) *Age and individual productivity: a literature survey*. In Feichtinger, G. (ed.) *Yearbook of Population Research*, 133-153. Vienna: Austrian Academy of Sciences Press.

Stevens, R. De Waegenaere, A. and Melenberg, B. (2011). 'Longevity risk and natural hedge potential in portfolios of life insurance products: The effect of investment risk', CentER Discussion Paper No. 2011-036.

van Groezen, B., Meijdam, L. and Verbon, H. (2005) 'Serving the old: ageing and economic Growth', *Oxford Economic Papers* 57(4): 647–663.

Wallis, K.F. (2003) 'Chi-Squared tests of interval and density forecasts, and the Bank of England's fan charts', *International Journal of Forecasting* 19(2): 165–175.

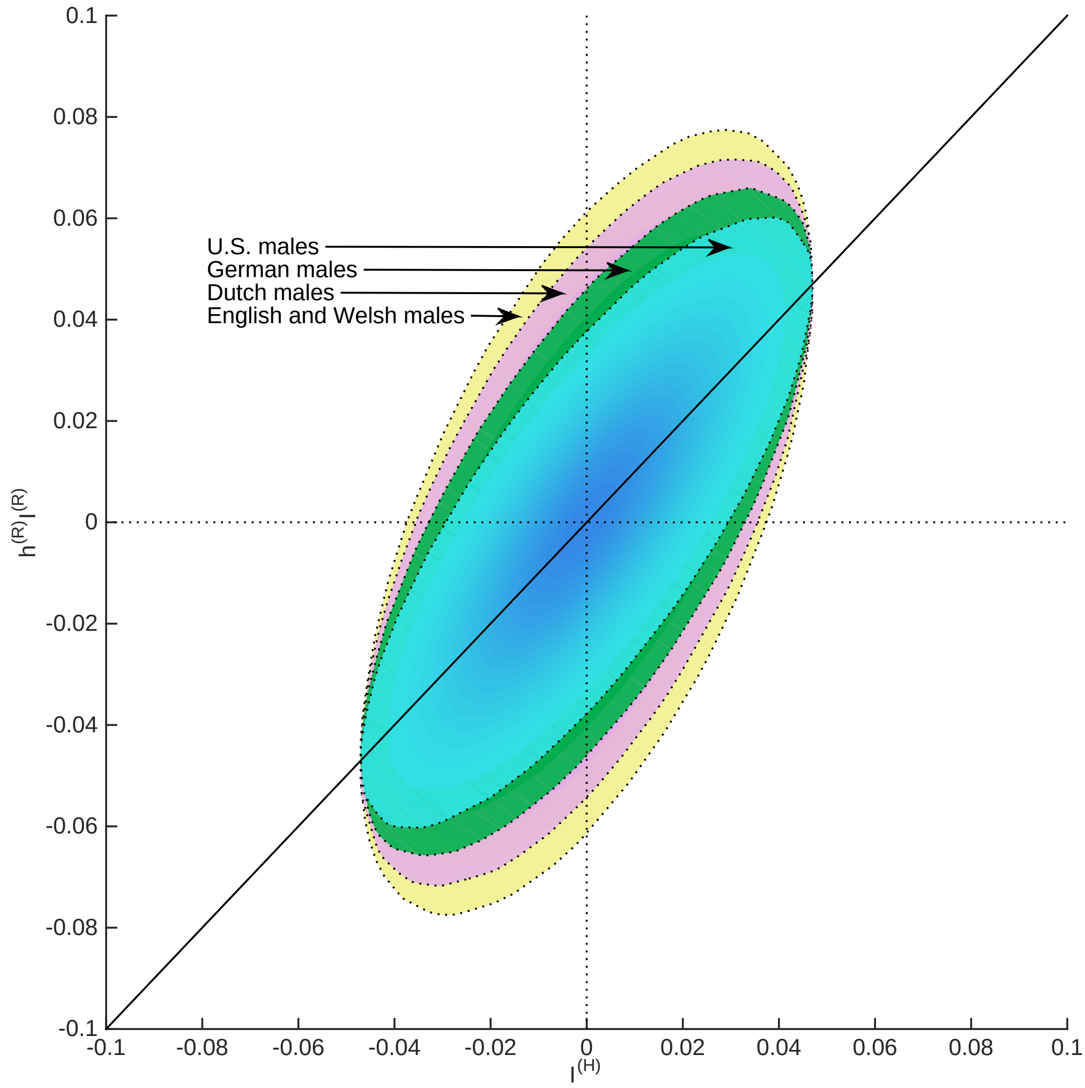

Figure 2: The graphical population basis risk metrics for the situations when the hedger's population (H) is Canadian males and the derivative's reference populations (R) are U.S. males, German males, Dutch males and English and Welsh males, respectively.